Lab on a Chip

RSC Publishing

PAPER

View Article Online
View Journal | View Issue

Published on 07 August 2013. Downloaded by Imperial College London Library on 17/05/2016 15:39:18.

Cite this: *Lab Chip*, 2013, **13**, 4173

Detection of real-time dynamics of drug–target interactions by ultralong nanowalls†

Andreas Menzel,‡*[a] Raphael J. Gübeli,‡[b] Firat Güder,[a] Wilfried Weber[b] and Margit Zacharias[ac]

Received 9th June 2013,
Accepted 5th August 2013

DOI: 10.1039/c3lc50694k

www.rsc.org/loc

Detecting drug–target interactions in real-time is a powerful approach for drug discovery and analytics. We show here for the first time the ultra fast electrical real-time detection and quantification of antibiotics using a novel biohybrid nanosensor. The biomolecular sensing is performed on ultralong (mm range) high aspect ratio nanowall (50 nm width) surfaces functionalized with operator DNA tetO which is specifically bound by the sensor protein TetR. This sensor protein is released from the operator DNA in a dose dependent manner by exposing the device functionalized with this bound DNA–protein complex to tetracycline antibiotics. As a result, the electrical conductance is accordingly modulated by these surface net charge changes. The switching mechanism of sensor proteins attached at the functionalized surfaces and releasing them again by antibiotics is demonstrated. With the here presented device the detection limit is below the limits of prevailing detection methods. Moreover, the study is extended to detect antibiotic residues in spiked organic milk from cows far below the maximum residual level of the European Union. In spiked milk samples a detection limit for tetracycline concentrations in the 100 fM level was achieved. The nanowall devices are fabricated by atomic layer deposition-based spacer lithography on full wafer scale which is a simple approach capable for mass production.

Introduction

Sensitive and reliable quantification and characterization of molecular events such as molecule–protein or protein–DNA interactions are of huge importance for the elucidation of drug actions,[1,2] detection of (harmful) substances,[3] and the understanding of complex biological networks.[4] Moreover, the real time monitoring of binding and releasing charged molecules like proteins from surfaces is still a difficult and lacking point and an electrical detection of such interactions based on a field effect transistor (FET) configuration was not reported, yet.

There exist some established techniques based on optical read out principles such as enzyme-linked immunosorbent assays (ELISA), surface plasmon resonance (SPR) detection or some chemometric techniques.[5–7] These techniques, however, have huge disadvantages in terms of time consumption due to long reaction times, cost expensive tools and reagents, labeling of molecules and limited sensitivity.[8] Electrochemical detection methods are reported but they are either limited in their detection or still take a long response time (~30 min) or require some additional magnetic beads.[9,10] Rapid label-free electrical detection systems could provide the ability of a strong sensitivity which can be obtained by the use of semiconducting nanostructured sensors due to their huge surface to volume ratio.[11,12] Field effect transistor devices with dimensions in the nanometer scale have the ability to provide a very sensitive detection because changes in the surface charge induce a strong band bending effect which changes the current in the material drastically compared to their bulk counterparts. Among the wide range of semiconducting materials, zinc oxide (ZnO)-based materials have shown promising characteristics as field effect transistors and optical, chemical, gas, and biological sensors.[13,14] While the approach to obtain ZnO NWs by thermal chemical vapor deposition (CVD) methods is nowadays a very common but still not very reliable technology,[15] we focus here on a ZnO thin film atomic layer deposition (ALD) based approach to fabricate the nanosensor platform. ALD has the advantage of fabricating arbitrary and high aspect ratio nanostructures over a large scale (*e.g.* wafer scale) in a very controlled way enabling mass fabrication of future nano-devices. The advantage of the here reported ALD based spacer lithography (ASL) is its variability in terms of material usage and dimension control.[16,17] The thickness dimension can be controlled down to Angstrom

[a]*Department of Microsystems Engineering – IMTEK, University of Freiburg, Germany. E-mail: andreas.menzel@imtek.uni-freiburg.de*
[b]*Faculty of Biology, Centre for Biological Signalling Studies (BIOSS) and Spemann Graduate School of Biology and Medicine (SGBM), University of Freiburg, Schänzlestrasse 1, 79104 Freiburg, Germany*
[c]*FRIAS, School of Soft Matter Research, University of Freiburg, Albertstraße 19, 79104 Freiburg, Germany*

† Electronic supplementary information (ESI) available. See DOI: 10.1039/c3lc50694k

‡ These authors contributed equally.

Published on 07 August 2013. Downloaded by Imperial College London Library on 17/05/2016 15:39:18.

range while the height of the structure can be controlled by the buried resist pattern which enables tremendous high aspect ratio (8 in this work but scaled by the resist to larger ratios) nanostructures on the wafer scale even as a batch processing as in our demonstration. ZnO in general has the advantage of its natural n-type semiconductor character which for the here discussed approach is a mandatory benefit.[18] Such low temperature fabrication methods allow a device fabrication ready for the field of "zero-cost" point-of-care (POC) diagnostics because the used processes and materials can be transferred to cheap polymer substrates and mass fabrication is possible.

The biofunctionalization of ZnO itself and the long term stability of the device in aqueous buffer solutions are challenging tasks. Groups have already tried to functionalize the ZnO surface with different target molecules; however, one major issue with ZnO is its photocorrosive instability in aqueous solutions.[19,20] A potential method to overcome this effect is the coating of the surface by a stable material based on another ALD step using the homogeneous growth of ALD layers over 3D nanostructures at low temperatures. We used here a thin layer of alumina (Al_2O_3) which enhances the long-term stability in aqueous solutions and at the same time can act as a dielectric for the field effect transistor.[21] Metal oxide surfaces like Al_2O_3 can be modified by organic ligands and exhibit high-k dielectric properties. Carboxylic acids as linkers have been shown to form a stable self assembled monolayer (SAM) on the surfaces.[22–25] Generally, the adsorption or desorption of negatively charged molecules on the Al_2O_3 gate oxide increases or decreases the surface charge which can be considered as a modulation of the liquid gate potential which can be explained by the surface band bending mechanism. Increasing the net surface charge leads to an up bending of the valence (E_V) and conduction (E_C) bands of ZnO nanowalls which has the effect of a decreased electrical conductance. The net charge is reduced when unbinding and removing of such negatively charged molecules from the surface occurs which reduces the band bending due to an accumulation layer at the ZnO surface. Hence, the conductance is increasing as a result.

In this study, we develop ultralong nanowalls as biosensors and demonstrate for the first time the real-time electrical measurement of dynamic molecular interactions. We apply the nanostructured device for the monitoring of the binding of the tetracycline repressor (TetR) to its operator DNA and its inducible release by the addition of tetracycline. This allows for ultra-sensitive measurements of tetracycline concentrations.

The suitability of this novel nano-structured device is shown by the exact quantification of tetracycline in an aqueous buffer solutions and complex biological samples such as milk. The rapid and simple detection of antibiotics in veterinary products is a very important issue these days. There is an overuse of antibiotics in veterinary products which is a risk to both animal and human health.[26] The electrical detection and quantification of residual antibiotics in real foodstuff is not only important from scientific point of view. Such a sensor as our here presented novel nanodevice FET configuration would open a way for an economic screening of the use of antibiotics if possible on real food samples. This motivated us to conduct measurements with the nanowall device in spiked organic milk samples from a local farmer. We will demonstrate the response to target antibiotic molecules (tetracycline) and the cross-sensitivity to other types of antibiotics like erythromycin, ampicillin and gentamicin.

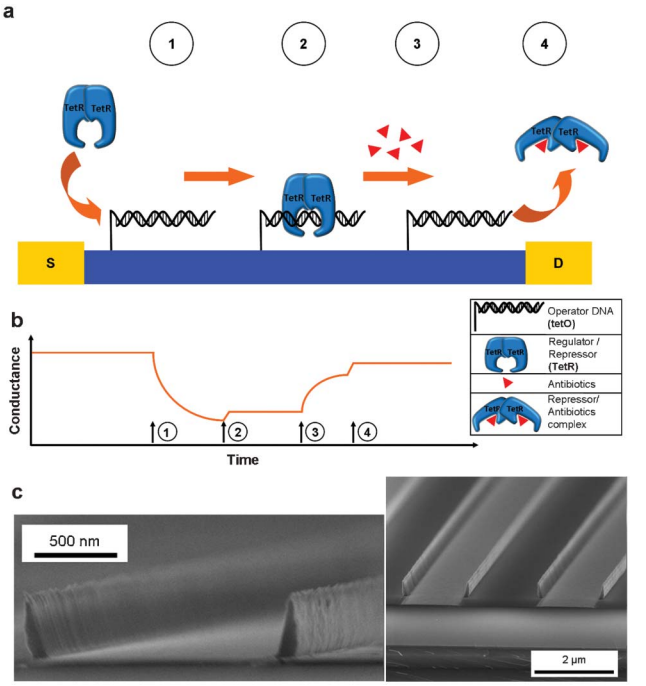

Fig. 1 Schematics of the label-free tetracycline detection on ZnO/Al_2O_3 nanowalls. (a) Switching mechanism on the Al_2O_3 surface. After immobilizing tetO on the ZnO/Al_2O_3 nanowall surface, TetR is bound to tetO. When adding tetracycline to the sensor surface TetR is released from tetO by an allosteric switching mechanism. (b) Electrical conductance (a.u.) mechanism of the n-type nanowalls. After tetO immobilization, the signal is detected in measurement buffer (steady state signal). The binding of TetR causes a reduction of the electrical conduction (1). Releasing TetR by tetracycline results in an increasing conduction (3). At time positions (2) and (4) the surface is washed and the device structure is measured in binding buffer solution. (c) SEM micrographs of the ASL nanowall device. The cross section of the nanowall device is shown.

Results and discussion

The general functional principle of the here presented device is shown in Fig. 1a. Details for the fabrication procedure for the ASL nanowall device are given below (Experimental section) and in the ESI† (Fig. S1). In this device configuration 1000 nanowalls are connected in parallel between source and drain contacts to enable a higher current throughput at a given applied voltage. Examples of the fabricated nanowalls are shown in Fig. 1c. The semiconductor nanowall device surface is first functionalized by double stranded operator oligonucleotides (tetO) composed of the minimal DNA sequence to which the tetracycline repressor protein (TetR) can bind in a

 This journal is © The Royal Society of Chemistry 2013

Published on 07 August 2013. Downloaded by Imperial College London Library on 17/05/2016 15:39:18.

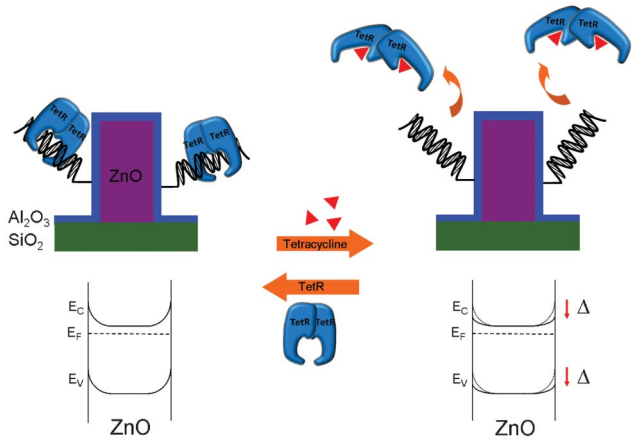

Fig. 2 Schematic energy band diagrams that show surface interactions on the ZnO/Al_2O_3 nanowall (cross section). The left image shows the functionalized nanowall device in the initial state. When tetracycline is added, the induced switching and release causes a down bending of the surface energy bands due to the reduction of negatively charged molecules. The process is reversed when TetR molecules are attached to the surface again. E_V and E_C are the valence and the conduction bands. E_F is the Fermi energy level.

very specific manner.[27] The here used tetO oligonucleotides include a carboxyl acid termination at the 5′ end of one strand. The electrical characteristics (Fig. 1b) like the source–drain conductivity (G_{DS}) is taken (step 1) after functionalization. While approaching the TetR to the DNA, there will be a charge transfer of adsorbing proteins and the conductivity decreases due to the n-type characteristics of ZnO (step 2).[28] The net charge of TetR is negative in the case of neutral (pH 7.8) surrounding buffer solutions and a corresponding isoelectrical point p*I* 6.2. A washing step removes the non-bound proteins and the signal is taken again which yields a slight increase in conductivity. When this functionalized device is then exposed to antibiotics of the tetracycline (TC) family (step 3), there will be an allosterically modulated conformational change in the protein structure. Hence, the TetR–TC complex is released from the tetO-modified sensor surface and reduces the amount of net surface charge bound on the sensor surface. A following washing step 4 is required to finally remove the nonbound TetR–TC complex from the device surface and the increased electrical conductivity is measured again. Fig. 2 shows a schematic diagram of the energy band bending on the nanowall surface (interface with bound molecules) in the case of a tetracycline induced switching event of TetR proteins. The left image is the initial case when TetR proteins are bound to the tetO functionalized nanowall surface. The energy bands are bent upwards in the diagram below. When the tetracycline molecules are added to the device (right image), TetR proteins release from the surface and reduce the amount of negative surface net charge. Thus, the energy bands at the surface are bent down and the electrical current is increased. If the device is loaded again with TetR proteins, the amount of negative surface net charge is increased again (left image) and the energy bands are lifted up again (reloading of the device).

For all the experiments the nano device was always exposed to a 0.1 mM binding buffer solution. One reason for this ionic strength binding buffer solution lies in the Debye screening effect to appropriately sense the protein–DNA interaction and the releasing effect of charged molecules on the nanostructured surfaces.[28,29] Only the charge of molecules that are present within the Debye length can be detected on the nanowall surface.

After successful functionalization (tetO) and blocking (BSA passivation) of the nanowall surfaces the device is ready for electrical measurements. The device is first loaded with the sensor protein by incubation in a solution containing 3 μg ml^{-1} TetR for 30 min and unbound TetR proteins are washed away with a washing step. The measurement necessitates a baseline measurement in pure binding buffer which is set as the reference line for the following electrical measurements. Next, the nanowall device was exposed to tetracycline ranging from 1 pM to 1 μM in decade steps in binding buffer. Thereby, the analyte is always washed with binding buffer after the tetracyclines were bound to TetR. Fig. 3a describes the entire time resolved-experimental procedure to obtain the dose response profile of the TetR-modified nanowalls to tetracycline. Time 0 s at step 0 describes the exposure of the nanowall device with bound TetR to binding buffer until a stable base line is reached. ZnO has a photocorrosive instability in aqueous solutions; however, the additional Al_2O_3 can overcome this challenge and a stable baseline can be achieved. Afterwards, 1 pM tetracycline in binding buffer is added to the system (step 1 in Fig. 3a) which yields to a rapid increase of the conductance (here absolute changes of conductance with respect to the baseline is shown). At this stage the tetracycline molecules bind the TetR protein leading to a conformational change of the TetR protein and the release of the tetracycline–TetR complex from its tetO binding sequence. The release from the nanowall surface is monitored and indicated by an increased value of G_{DS}. An additional washing step W (wash and measurement in binding buffer) after a 2 min incubation yields a further increase in conductance because the dissociated tetracycline–TetR complex is not present in the nanostructure surface environment any more (the conductance measurement after washing is again 2 min). From this point the tetracycline dose in binding buffer is increased in decades up to 1 μM (indicated by steps 2, 3, 4, 5, 6 and 7 in Fig. 3a). In between these steps the device is always rinsed with binding buffer and measured in the same for 2 min. It is noteworthy to observe that the sensor response below 0.1 nM is quite small, but still detectable. From 0.1 nM the response is much stronger and reaches saturation beyond 10 nM as most of the proteins are already expected to be unbound and released from the sensor surface. The data are summarized in Fig. 3b in a logarithmic scale. By fitting this plot with a dose response function ($G = G_{max}[c]_{TC}/(K_{ass}^{-1} + [c]_{TC})$) an association constant K_{ass} in the 10^9 M^{-1} range can be determined which agrees very well with data described in the literature for this TetR–tetracycline interaction system.[27,30] Please note that G_{max} is the maximum electrical conductance, $[c]_{TC}$ is the tetracycline

Published on 07 August 2013. Downloaded by Imperial College London Library on 17/05/2016 15:39:18.

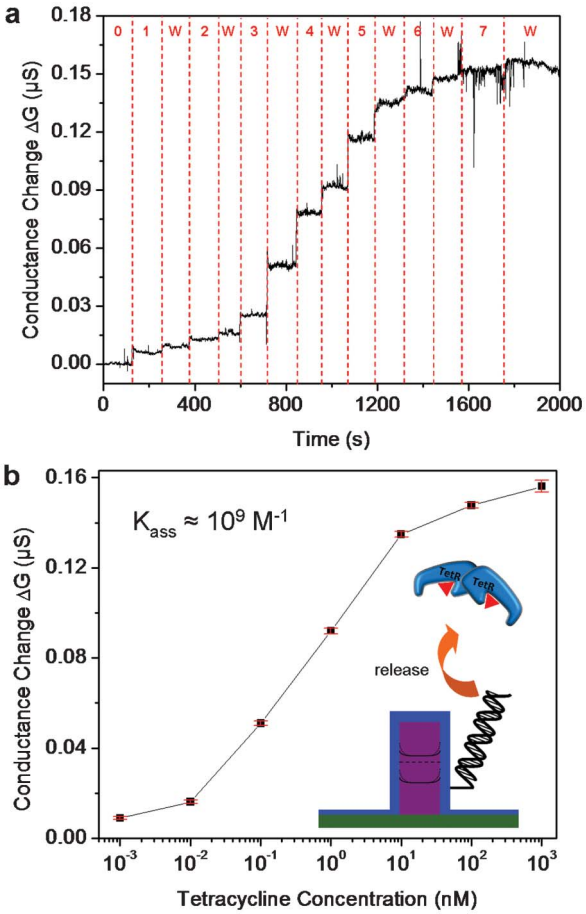

Fig. 3 Time-resolved and dose response conductance measurement (log scale) of tetracycline in measurement/binding buffer. (a) Tetracycline is injected into the measurement cell/device in concentrations ranging from 1 pM to 1 μM (steps 1 to 7). After each incubation, the device surface is washed and conductance is measured in binding buffer (indicated as step W). (b) Dose response summary with an association constant K_{ass} in the range of $10^9\ M^{-1}$.

concentration within the dose response function equation. More important is the point that this device is capable to electronically detect residues of tetracycline lower than 1 pM which is far below the European Union (EU) maximum residue level (MRL) of 100 μg kg^{-1} (225 nM) and makes the here reported measurement method much more sensitive than common methods such as enzyme-linked immunosorbed assays (ELISA) which have typical limits in the nM range.[31,32] We have performed ELISA experiment for verification that the tetracycline and TetR system works well for both buffer solutions and spiked milk samples (see also Fig. S2 in the ESI†). These experiments demonstrate the detection limit to be in the nM range. Thus, our nanowall device demonstrates a strong increase in sensitivity compared to other conventionally available devices to detect such drug–target interactions.

It is important for a future sensor device to have reliable and repeatable system characteristics. Furthermore, it is needed to demonstrate that we are able to investigate the switching mechanism of bound proteins to the operator DNA

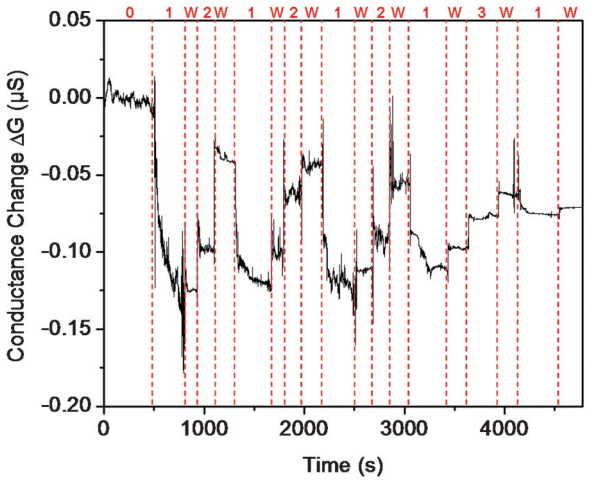

Fig. 4 Test of reversibility of the device. The electrical conductance measurement of the device is shown. In step 0 from 0 s to around 500 s the device is exposed to binding buffer and the baseline is recorded. The TetR proteins are incubated (step 1) and released by adding 50 nM (steps 2) and 10 nM (step 3) tetracycline to the system. This process is preceded four times by adding TetR proteins (steps 1) before releasing. Washing steps and measurement in binding buffer are indicated as steps W.

and releasing them again by antibiotics. In the following experiment shown in Fig. 4 the tetO-modified nanowall device is frequently exposed to TetR and tetracycline. In step 0 the electrical conductivity of the functionalized device is measured in binding buffer until a stabilized baseline is reached. Then, 3 μg ml^{-1} of TetR proteins dissolved in binding buffer were added and the conductance decreases during an incubation time of around 6 min (step 1). A washing step and conductance measurement directly after the incubation was done (step W). Subsequently, 50 nM tetracycline in binding buffer was added (step 2), the dissociated tetracycline–TetR complex was washed away and the conductance of the system was measured in binding buffer as indicated in step W. A subsequent TetR incubation and tetracycline-mediated removal was carried out two more times to demonstrate the switching effect and the repeatability of the device. The final step 3 was done to detect a lower concentration of 10 nM of tetracycline and there was still a change in conductance observable which shows that the device still works properly. However, the strength of the response is decreasing over the cycles which can potentially be attributed to the accumulation of unspecifically binding proteins.

After successfully demonstrating the quantification of the tetracycline concentration by the nanowall device with high sensitivity the device is next subjected to a real-world application which is the detection and quantification of antibiotic residues in veterinary products (*e.g.* milk).

Here, the detection of tetracycline in milk and the cross sensitive effects to other typical antibiotic classes will be shown. For this experiment raw milk from German cows (organic farming) without any antibiotic contamination was taken. The milk was then separated in different sample tubes

 This journal is © The Royal Society of Chemistry 2013

Published on 07 August 2013. Downloaded by Imperial College London Library on 17/05/2016 15:39:18.

and spiked with different exemplified antibiotic classes (tetracycline, erythromycin, ampicillin, and gentamicin) in concentrations according to the MRL of the EU. The MRL are 100 μg L^{-1}, 40 μg L^{-1}, 4 μg L^{-1}, and 100 μg L^{-1} for tetracycline, erythromycin, ampicillin, and gentamicin, respectively.[31,33–35] However, milk in general contains a typical ionic strength of around 220 mM due to its mineral composition (Ca, Fe, Mg, P, Na, *etc.*).[36] Thus, the milk has to be diluted to obtain the required ionic strength of 0.1 mM which has the consequence of a 3 orders dilution of the antibiotics concentration. In Fig. 5a, the cross sensitivity is first tested by exposing the device to the different spiked milk solutions. The steps W correspond always to the binding buffer washing steps and measurements in binding buffer and step 0 shows the initial baseline measurement. In step B, bare (un-spiked) diluted organic milk in binding buffer was introduced into the measurement cell and no effect of the washing was observed. Then, the diluted milk containing erythromycin, ampicillin, gentamicin was introduced in steps E, A, and G, respectively. No significant changes in the electrical conductance were observable which shows that the TetR protein does not respond to other antibiotic classes than tetracycline. When exposing the device to the gentamicin sample, only a low signal response is observable. Since the signal turns back after washing the device, the signal change can be attributed to a non-specific adsorption of gentamicin on the sensor surface which does not affect the TetR proteins.

Tetracycline spiked milk samples were then added in the same manner which corresponds to concentrations ranging between 100 fM to 100 pM after a 2000-fold dilution which represents the diluted MRL. The experiment in Fig. 5a is extended to the mentioned dose response profile which includes the steps 1 to 4 for respective applied concentrations. Here, the steps W always correspond to washing steps and measurement in binding buffer. We observe a slight increase of the signal over time which can be attributed to the low concentrated amount of tetracycline present in the milk and the bound complex of tetracycline in the milk matrix (*e.g.* with Ca^{2+} ions) which reduces the binding kinetics. Ca^{2+} ions bind with tetracycline which leads to a reduced affinity to bind with TetR. However, the affinity is still strong enough to detect these molecules by our sensor structure. The averaged dose response data of tested milk samples are summarized in Fig. 5b (logarithm scale) and show a similar responsiveness as the dose response profile in Fig. 3b using buffer alone. By the here presented experiments we demonstrate for the first time a simple fabrication of a nanowall device which can be applied to rapidly detect ultra low concentrations of residual tetracycline antibiotics in a real biological system like milk.

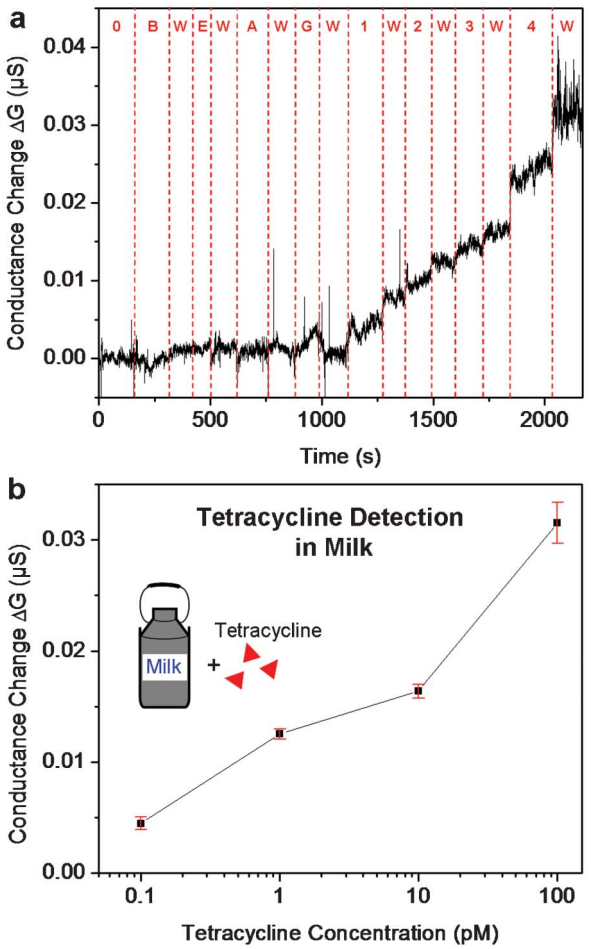

Fig. 5 Time-resolved and dose–response conductance measurement (log scale) of spiked milk. Additionally, the cross sensitivity of the device is shown. (a) Step 0 represents the baseline of the conductivity. In steps B, E, A and G the device is exposed to bare milk (B) and erythromycin (E), ampicillin (A), and gentamicin (G) according to the maximum residual levels of the European Union. Washing steps are indicated as W. Spiked milk samples with 0.1 pM to 100 pM tetracycline are detected in steps 1 to 4. (b) Dose response summary for tetracycline spiked milk samples in the range between 0.1 pM to 100 pM.

Conclusions

In summary, we fabricated an ultralong and high aspect ratio ZnO/Al_2O_3 nanowall FET device. In this study we pioneered a new concept for electrically quantifying drug–target interactions in real time and have shown its applicability for detecting tetracycline antibiotics in milk. Generally, the electrical readout of our devices realizes detection limits far below the prevailing detection limits by, such as, ELISA, SPR, *etc*. The impact of this study is likely to go far beyond this specific application as TetR stands for a whole family of proteins (the TetR family) that specifically bind a cognate DNA operator sequence in response to most diverse small molecules like drugs, metabolites, vitamins or metals.[37,38] Therefore, by simply replacing TetR–tetO with a different protein–DNA pair, the technology described in this study can be adapted to quantify most diverse small molecule compounds. This quantification can be used as a highly sensitive and fast analytical assay, however, given the importance of switchable protein–DNA interactions in drug discovery[39,40] we also anticipate the here-described method as a miniaturized

Published on 07 August 2013. Downloaded by Imperial College London Library on 17/05/2016 15:39:18.

tool in the high-throughput, multiparallel screening for new drug candidates.

The switching mechanism of binding and releasing proteins as well as the repeatability and reliability are shown by exposing the device several times to TetR proteins and tetracycline. The corresponding surface band bending mechanism was measured here by the electrical conductance. The electrical source drain conductance was continuously taken and concentrations ranging between 1 pM to 1 μM were detected while a typical association constant K_{ass} of around 10^9 M^{-1} was determined. We repeated the test with other nanowall samples which show similar device characteristics.

Milk experiments with diluted bare milk, and milk spiked in a controlled way with TetR specific tetracycline as well as with antibiotics of other classes are reported. Bare milk and antibiotics of other classes have shown a negligible response to TetR which demonstrates a weak cross sensitivity of the sensor system. Tetracycline spiked milk samples according to the maximum residue levels by the EU were tested in a diluted form and concentrations down to the 100 fM were successfully detected by the nanowall FET device which demonstrates that the device is ready for quantification of antibiotics.

Experimental section

Fabrication of ASL based nanowall device

The fabrication procedure for the ASL nanowall device is shown in Fig. S1 (ESI†) and starts with a 1 μm thick SiO_2 dielectric layer on a Si (100) wafer. High resolution TSMR photo resist coating and standard photolithography with UV exposure and development in MIF 726 is followed to obtain parallel rectangular (resist) stripes with extremely vertical side walls (400 nm height) over the full wafer (cm range). Next, 50 nm polycrystalline ZnO is 3-dimensionally deposited over the stripes by a low temperature ALD process (115 °C, DEZ precursor) to obtain a homogeneous layer. Reactive ion etching (RIE) is carried out to anisotropically etch on top of the stripes and on the substrate bottom the 50 nm ZnO away such that only the ZnO at the photo resist stripes sidewalls remain. An additional oxygen plasma process step (at 220 °C) removes the resist stripes and free standing ZnO nanowalls (Fig. 1c) are obtained. The height and thickness (aspect ratio) of nanowalls can be controlled by the height of the resist lines and the ALD deposited thickness, respectively. A large scale top view as well as a cross sectioned view of the ASL device can be found in Fig. S1b, ESI†). Metal evaporation of a 400 nm Al and 100 nm Au layer is followed to obtain electrical source and drain contacts. Afterwards, the gate dielectric layer of Al_2O_3 is formed by an additional ALD process step (200 °C, TMA precursor). The nanowall devices are then electrically connected by Al wire bonding and electrically passivated by PDMS.

Production of the TetR protein

The DNA-binding protein TetR was produced according to ref. 41. Shortly, *E. coli* BL21* (DE3) pLysS cells were transformed with the plasmid pWW307 for expression of a C-terminally hexahistidine-tagged TetR protein and protein expression was induced in LB medium at OD_{600} = 1 with 1 mM isopropyl β-D-1-thiogalactopyranoside (IPTG) for 4 h at 37 °C. The cells were centrifuged (6000 × *g*, 7 min, 4 °C) and resuspended in lysis buffer (40 ml per 1000 ml initial culture volume, 50 mM NaH_2PO_4, 300 mM NaCl, 10 mM imidazole, pH 8.0), disrupted using a French press (1000 bar, 3 passages, APV, DK, Albertslund, APV-2000) and cell debris was eliminated by centrifugation at 30 000 × *g* for 30 min at 4 °C. The lysate was loaded onto a gravity flow Ni^{2+}-NTA-agarose Superflow column (10 ml lysate per ml Ni^{2+}-NTA-agarose bead volume, Qiagen, Hilden, Germany, cat. no. 30210) following washing with 10 column volumes lysis buffer, 10 column volumes wash buffer (50 mM NaH_2PO_4, 300 mM NaCl, 20 mM imidazole, pH 8.0) and elution with 2 column volumes elution buffer (50 mM NaH_2PO_4, 300 mM NaCl, 250 mM imidazole, pH 8.0). After addition of 10% sucrose, the TetR protein was concentrated to 0.6 mg ml^{-1}, freeze-dried and stored at −80 °C. For experiments, the lyophilized TetR protein was dissolved by the addition of H_2O. The protein concentration was determined by the Bradford method (Bio-Rad, Hercules, CA, cat. No. 500-0006) with bovine serum albumin (BSA) as standard.

Annealing of the carboxyl acid terminated double stranded oligonucleotides (tetO)

For the generation of double-stranded operator DNA for the binding of the TetR protein, the oligonucleotides oRG128 (5′-actccctatcagtgatagagaaa-3′) and oRG229 (5′-tttctctatcactgatagggagt-3′, 5′-COOH functionalized from IBA GmbH (Göttingen, Germany), cat. no. 5-0210-23X) were mixed in equimolar amounts (50 μM of each oligonucleotide) in 1 × SSC buffer (15 mM sodium citrate, 150 mM NaCl, pH 7), incubated at 95 °C for 5 min followed by slowly cooling down (2 °C per min) to room temperature.

Functionalization procedure

Each device was functionalized for 2 h by carboxyl acid-terminated double stranded tetO oligonucleotides (tetO). The device was then rinsed in DI water to remove non-bound molecules. 1% (v/v) Bovine serum albumin (BSA, Sigma Aldrich, cat. no. 05479) in 0.1 mM binding buffer (diluted from stock solution: 50 mM Tris, 20 mM $MgCl_2$ and 250 mM NaCl, pH 7.8) was added for 30 min to block non-specifically protein binding surface areas. From ELISA experiments an incubation time of 30 min has shown that TetR proteins bind already well to the tetO. Demonstration examples for the tetracycline detection in buffer and milk samples by ELISA methods are shown in the ESI† (see Fig. S2).

Antibiotics preparation procedure

Tetracycline was obtained from Applichem (AppliChem, Darmstadt, Germany, cat. no. A1685,0025) and dissolved as a 2 mg ml^{-1} stock solution in ethanol. Erythromycin was obtained from Sigma-Aldrich (cat. no. E-5389) and dissolved as a 10 mg ml^{-1} stock solution in ethanol. Ampicillin was obtained from Roth (Carl Roth, Karlsruhe, Germany, cat. no. K029.2) and dissolved as a 100 mg ml^{-1} stock solution in H_2O. Gentamycin was obtained from Enzo Life Sciences (Enzo Life Sciences, Lausen, Switzerland, cat. no. 380-003-G005) and

 This journal is © The Royal Society of Chemistry 2013

Published on 07 August 2013. Downloaded by Imperial College London Library on 17/05/2016 15:39:18.

dissolved as a 20 mg ml^{-1} stock solution in H_2O. The stock solutions were diluted in binding buffer or milk (organic farming) to the final experimental concentration.

Electrical measurement setup

The prepared and functionalized devices are connected with a high precision Keithley 2636 source meter which is connected to a personal computer by USB. The continuous and time-dependent measurements were recorded by the LabView program.

Acknowledgements

We thank Dr Kittitat Subannajui for fruitful discussions. This work was supported by the Freiburg Institute for Advanced Studies (FRIAS), the European Research Council under the European Community's Seventh Framework Program (FP7/2007-2013)/ERC Grant agreement n° 259 043-CompBioMat and the Excellence Initiative of the German Federal and State Governments (EXC-294 and GSC-4). M.Z. acknowledges the DFG for funding (ZA191/24-1).

References

1 C. Baldock, J. Rafferty, S. Sedelnikova, P. Baker, A. Stuitje, A. Slabas, T. Hawkes and D. Rice, *Science*, 1996, **274**, 2107–2110.
2 J. Overington, B. Al-Lazikani and A. Hopkins, *Nat. Rev. Drug Discovery*, 2006, **5**, 993–996.
3 Y. Xiang and Y. Lu, *Nat. Chem.*, 2011, **3**, 697–703.
4 S. Hu, Z. Xie, A. Onishi, X. Yu, L. Jiang, J. Lin, H. Rho, C. Woodard, H. Wang, J. Jeong, S. Long, X. He, H. Wade, S. Blackshaw, J. Qian and H. Zhu, *Cell*, 2009, **139**, 610–622.
5 N. Moeller, E. Mueller-Seitz, O. Scholz, W. Hillen, A. Bergwerff and M. Petz, *Eur. Food Res. Technol.*, 2007, **224**, 285–292.
6 O. Nagel, M. Molina and R. Althaus, *Lett. Appl. Microbiol.*, 2011, **52**, 245–252.
7 P. Zijlstra, P. Paulo and M. Orrit, *Nat. Nanotechnol.*, 2012, **7**, 379–382.
8 M. Piliarik and J. Homola, *Opt. Express*, 2009, **17**, 16505–16517.
9 E. Zacco, J. Adrian, R. Galve, M.-P. Marco, S. Alegret and M. I. Pividori, *Biosens. Bioelectron.*, 2007, **22**, 2184–2191.
10 G. E. Pellegrini, G. Carpico and E. Coni, *Anal. Chim. Acta*, 2004, **520**, 13–18.
11 Y. Cui, Q. Wei, H. Park and C. M. Lieber, *Science*, 2001, **293**, 1289–1292.
12 F. Patolsky, G. Zheng, O. Hayden, M. Lakadamyali, X. Zhuang and C. M. Lieber, *Proc. Natl. Acad. Sci. U. S. A.*, 2004, **101**, 14017.
13 A. Menzel, K. Subannajui, F. Güder, D. Moser, O. Paul and M. Zacharias, *Adv. Funct. Mater.*, 2011, **21**, 4342–4348.
14 N. S. Ramgir, Y. Yang and M. Zacharias, *Small*, 2010, **6**, 1705–1722.
15 A. Menzel, R. Goldberg, G. Burshtein, V. Lumelsky, K. Subannajui, M. Zacharias and Y. Lifshitz, *J. Phys. Chem. C*, 2012, **116**, 5524–5530.
16 K. Subannajui, A. Menzel, F. Güder, Y. Yang, K. Schumann, X. Lu and M. Zacharias, *Adv. Funct. Mater.*, 2013, **23**, 191–197.
17 K. Subannajui, F. Güder, J. Danhof, A. Menzel, Y. Yang, L. Kirste, C. Wang, V. Cimalla, U. Schwarz and M. Zacharias, *Nanotechnology*, 2012, **23**, 235607.
18 Ü. Özgür, Y. Alivov, C. Liu, A. Teke, M. Reshchikov, S. Dogan, V. Avrutin, S. Cho and H. Morkoc, *J. Appl. Phys.*, 2005, **98**, 041301.
19 A. Choi, K. Kim, H. Jung and S. Lee, *Sens. Actuators, B*, 2010, **148**, 577–582.
20 Y. Yang, D. Kim, Y. Qin, A. Berger, R. Scholz, H. Kim, M. Knez and U. Gösele, *J. Am. Chem. Soc.*, 2009, **131**, 13920–13921.
21 S. Chen, J. G. Bomer, E. T. Carlen and A. van den Berg, *Nano Lett.*, 2011, **11**, 2334–2341.
22 A. Ulman, *Chem. Rev.*, 1996, **96**, 1533–1554.
23 M. Neouze and U. Schubert, *Monatsh. Chem.*, 2008, **139**, 183–195.
24 D. Allara and R. Nuzzo, *Langmuir*, 1985, **1**, 45–52.
25 D. Allara and R. Nuzzo, *Langmuir*, 1985, **1**, 52–66.
26 N. Gilbert, *Nature*, 2012, **481**, 125.
27 P. Orth, D. Schnappinger, W. Hillen, W. Saenger and W. Hinrichs, *Nat. Struct. Biol.*, 2000, **7**, 215–219.
28 K. Bradley, M. Briman, A. Star and G. Grüner, *Nano Lett.*, 2004, **4**, 253–256.
29 S. Sorgenfrei, C. Chiu, M. Johnston, C. Nuckolls and K. Shepard, *Nano Lett.*, 2011, **11**, 3739–3743.
30 S. Kedracka-Krok, A. Gorecki, P. Bonarek and Z. Wasylewski, *Biochemistry*, 2005, **44**, 1037–1046.
31 EMEA, The European Agency for the Evaluation of Medicinal Products, Committee for Veterinary Medicinal Products. Oxytetracycline, Tetracycline, Chlortetracycline, Summary Report (3) 1995, EMEA/MRL/023/95.
32 C. C. Weber, N. Link, C. Fux, A. Zisch, W. Weber and M. Fussenegger, *Biotechnol. Bioeng.*, 2005, **89**, 9–17.
33 EMEA, The European Agency for the Evaluation of Medicinal Products, Committee for Veterinary Medicinal Products. Erythromycin, Summary Report (3) 2002, EMEA/MRL/821/02-Final.
34 EMEA, European Medicines Agency, Committee for Veterinary Medicinal Products. Penicillins, Summary Report 2008, Revision 1.
35 EMEA, European Medicines Agency, Committee for Veterinary Medicinal Products. Gentamicin, Summary Report (1) 2002, EMEA/MRL/003/95.
36 E. Medhammar, R. Wijesinha-Bettoni, B. Stadlmayr, E. Nilsson, U. Charrondiere and B. Burlingame, *J. Sci. Food Agric.*, 2012, **92**, 445–474.
37 J. Ramos, M. Martínez-Bueno, A. Molina-Henares, W. Terán, K. Watanabe, X. Zhang, M. Gallegos, R. Brennan and R. Tobes, *Microbiol. Mol. Biol. Rev.*, 2005, **69**, 326–356.
38 E. Christen, M. Karlsson, M. Kämpf, R. Schoenmakers, R. J. Gübeli, H. Wischhusen, C. Friedrich, M. Fussenegger and W. Weber, *Adv. Funct. Mater.*, 2011, **21**, 2861–2867.
39 W. Weber, R. Schoenmakers, B. Keller, M. Gitzinger, T. Grau, M. Daoud-El Baba, P. Sander and M. Fussenegger, *Proc. Natl. Acad. Sci. U. S. A.*, 2008, **105**, 9994–9998.
40 W. Weber and M. Fussenegger, *Nat. Rev. Genet.*, 2012, **13**, 21–35.
41 E. Christen, M. Karlsson, M. Kämpf, C. C. Weber, M. Fussenegger and W. Weber, *Protein Expression Purif.*, 2009, **66**, 158–164.